

## Parametric study of manufacturing ultrafine polybenzimidazole fibers by electrospinning

S. Anandhan · K. Ponprapakaran · T. Senthil · Gibin George

Received: 21 July 2012 / Accepted: 4 September 2012 / Published online: 16 September 2012  
© Central Institute of Plastics Engineering & Technology 2012

**Abstract** Polybenzimidazole (PBI), a high performance polymer, was synthesized from 3,3'-diaminobenzidine (DAB) and isophthalic acid (IPA) through polycondensation. The chemical structure of PBI was confirmed by Fourier transform infrared spectroscopy. Thermal characterization of PBI was done by thermogravimetry and differential scanning calorimetry. PBI nanofibers were fabricated by electrospinning of N, N-dimethyl acetamide solutions of PBI of different solution concentrations, at different voltages. The effects of solution and process parameters (namely, solution concentration and DC voltage) on morphology and average diameter of electrospun PBI fibers were investigated. The electrospun ultrafine fibers' diameter and morphology were characterized by using scanning electron microscopy. Nanofibers were obtained only from PBI solutions of concentrations 12 and 14 % (w/v). At concentrations of 8, 10, and 16 %, fibers could not be obtained. The process parameters were optimized by using the statistical tool, factorial or two-way ANOVA (analysis of variance), DOE (design of experiments) and the results indicate that the applied voltage and the interaction of voltage and solution concentration are influential in determining the diameter and morphology of the electrospun ultrathin PBI fibers. Electrospun PBI fibers, as small as 56 nm, could be successfully produced by using the right combination of solution concentration and spinning voltage.

**Keywords** PBI · Electrospinning · Nanofiber · ANOVA · Optimization

---

S. Anandhan (✉) · K. Ponprapakaran · T. Senthil · G. George  
Department of Metallurgical and Materials Engineering, National Institute of Technology Karnataka,  
Srinivas Nagar, Mangalore 575025, India  
e-mail: anandtmg@gmail.com

S. Anandhan  
e-mail: anandhan@nitk.ac.in

## Introduction

Electrospinning is used to produce polymeric fibers with diameters in the range of 3 nm to 20  $\mu\text{m}$  [1]. Electrospinning involves the use of high electrical voltage (10–50 kV) to charge the surface of a polymer droplet and thus induce the ejection of a liquid jet through a spinneret [2]. Morphology and diameter of electrospun fibers are affected by solution parameters, such as concentration, viscosity, conductivity and surface tension, in addition to process parameters, including applied voltage, flow rate and distance between spinneret tip and collector. Hence, both the solution and process parameters need to be optimized to produce defect-free ultrathin nanofibers [3, 4].

Neo et al. [5] investigated the effects of solution and processing parameters on electrospun zein fibers. Response surface methodology (RSM) analysis performed by them indicated that electrospinning parameters like solution concentration, applied voltage and flow rate have significant impact on the average fiber diameter (AFD) and also revealed that polymeric solution concentration was the most significant parameter compared to the others. Sukigara et al. [6] found that solution concentration had a great impact in controlling diameter of electrospun *bombyx mori* silk fibers. An orthogonal experimental design was utilized by Cui et al. [7], who investigated qualitative and quantitative correlations between poly(DL-lactide) fiber processing and materials parameters. The parameters used in the above-mentioned, showed that polymer molecular weight and solution concentration were significant influences on fiber diameter and morphology. Zamri et al. [8] used analysis of variance (ANOVA) method to prove that the low surrounding temperature (18 °C) was inducing the formation of stable nanofibers of poly(vinyl alcohol)/MWCNT/MnO<sub>2</sub> composite. In addition, the central composite design (CCD) and RSM methods were used to optimize the electrospinning process. Factorial design method, since it enables reduced number of experimental runs, was used to optimize the influence of the operating parameters to control the diameter of electrospun polycaprolactone fibers, by Khan et al. [9].

High performance polymers have attracted a great deal of attention due to their amazing properties, such as high radiation and heat resistance, good mechanical strength and electrical properties, and excellent thermo-oxidative and thermal stability [10]. Electrospun high performance polymer nanofibers have attractive applications in areas such as nuclear power, aeronautics, heat-resistant membranes, micro-electronics, flame-retardant materials, etc. due to their outstanding properties [11, 12].

Zhang et al. [13] reported the preparation of polyimide nanofibers by electrospinning. The morphology of the resultant fibers showed that larger fiber diameter distributions (> 300 nm) were related to a high solution concentration. Moon et al. [14] examined the effect of process and solution parameters of electrospinning of a polyetherimide from 1-methyl-2-pyrrolidinone. Nakata et al. [15] prepared poly(ether sulfone) nanofibers web for developing heat-resistant high performance air filter. They showed that the fiber diameter, pore size and filtration properties depended on operating parameters such as vapor pressure, viscosity of solution, applied voltage and flow rate. Solution concentration and flow rate were found to have relatively larger effects on the fiber diameter and pore size than the other parameters.

PBI is a high performance polymer, which has potential applications in high temperature atmospheres, and it exhibits excellent heat and wear resistance, excellent ultrasonic transparency, mechanical properties and load carrying capability at extreme

temperatures than any other engineering plastics [16]. Therefore, aromatic heterocyclic PBI plays an important role in advanced applications, such as semiconductor, automotive, aircraft and aerospace materials [17].

The first attempt to electrospin PBI was by Kim and Reneker [18]. However, the ultrafine fibers produced by them had an average diameter of 300 nm. Since then, there has been no report on preparation of ultrafine PBI nanofibers of diameters less than 100 nm or so. In this study, we report the synthesis of PBI fibers of average diameters as small as 50 nm by electrospinning. The effect of solution and process parameters on the morphology and size of PBI nanofibers was examined. It was noticed that significant changes in fiber diameter and morphology accompany changes in these parameters. We used two-way ANOVA to determine the major factors and interactions that significantly affect the fiber diameter and morphology.

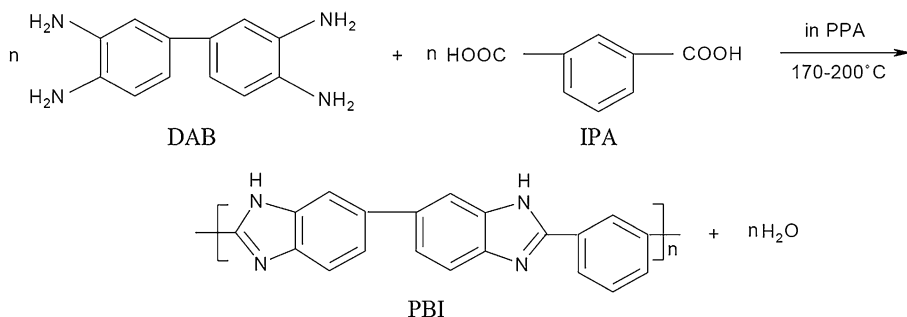
## Experimental

### Materials

DAB was purchased from Sisco research laboratories Pvt. Ltd., India; IPA was procured from Sigma-Aldrich, Germany; poly(phosphoric acid) (PPA) obtained from Spectrochemical Pvt. Ltd., India was used as the reaction medium; N,N-dimethylacetamide (DMAc), the solvent for the electrospinning of PBI, was procured from HPLC Pvt. Ltd., India; sodium bicarbonate was obtained from RFCL Ltd., India; sulfuric acid and methanol were supplied by Nice chemicals Pvt. Ltd., India. All the chemicals were of highest analytical purity and used without any further purification.

### Synthesis of PBI

PBI was synthesized according to the procedure reported earlier by Ainla and Brandell [19]. The chemical equation for the synthesis is shown in Scheme 1. 1 g of DAB and 15 g of PPA were added into a round bottom flask equipped with a magnetic stirrer. The solution was heated to 180 °C under a N<sub>2</sub> stream to dissolve DAB in PPA. 0.75 g of IPA was then added and the temperature was raised to 200 °C. After 17 h, the highly viscous and dark brown colored solution was poured into a large amount of cold water. It was kept in water for 2 days. The excess acid was



**Scheme 1** Reaction scheme for the synthesis of PBI

neutralized with an aqueous solution of sodium bicarbonate. The polymer was then collected by filtration, washed thoroughly with water and methanol, and then dried under a vacuum at 60 °C for 24 h.

## Characterization of PBI

### *Determination of viscosity average molecular weight*

The molecular weight of PBI was determined at 25 °C by viscometry [20], with PBI solutions of concentrations 0.1, 0.3, 0.5, 0.7 % (w/v) in 97 % sulfuric acid. The viscosity average molecular weight ( $\overline{M}_v$ , in  $\text{g}\cdot\text{mol}^{-1}$ ) was calculated by the Mark-Kuhn-Houwink equation [20]:

$$[\eta] = K\overline{M}_v^a \quad (1)$$

Where,  $[\eta]$  is intrinsic viscosity;  $K$  and  $a$  are constants that depend on the polymer, solvent and temperature. The values of  $K$  and  $a$  at 25 °C for PBI dissolved in sulfuric acid, are  $1.94 \times 10^{-4}$  and 0.791, respectively [21].

### *Fourier transform infrared spectroscopy*

PBI was mixed with KBr and made into a pellet by using a hydraulic press. The FTIR spectrum of this pellet was taken in transmission mode by using a FTIR spectrometer (Thermo, Nicolet Avatar 330). The scans were made in a wave number range from 400 to  $4,000 \text{ cm}^{-1}$  and the average of 32 scans was recorded.

### *Thermogravimetry*

Thermal stability of PBI was determined by using a thermogravimetric analyzer (EXSTAR 6000 TG/DTA 6300, Japan). The sample (~8 mg) was placed in a platinum crucible and heated from 30 to 900 °C at a heating rate of  $10 \text{ }^\circ\text{C}\cdot\text{min}^{-1}$ , under a dynamic nitrogen atmosphere flowing at  $50 \text{ mL}\cdot\text{min}^{-1}$ .

### *Differential Scanning Calorimetry*

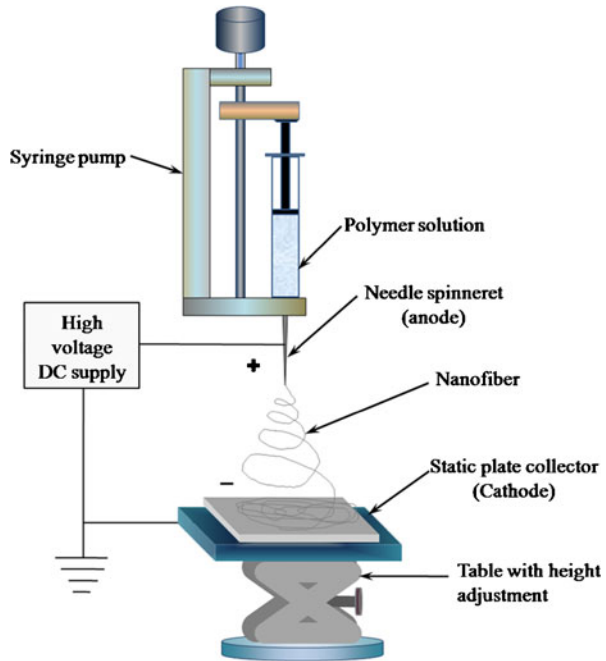
DSC analysis was carried out in a differential scanning calorimeter (Shimadzu DSC-60, Japan). Typically, a sample of about 10 mg was heated under a nitrogen atmosphere (flow rate  $50 \text{ mL}\cdot\text{min}^{-1}$ ) from 30 °C to 500 °C at a heating rate of  $10 \text{ }^\circ\text{C}\cdot\text{min}^{-1}$ .

## Electrospinning of PBI and characterization of the electrospun products

Electrospinning was carried out by using a vertical electrospinning setup (E-spin Nano, Physics Equipments Co., India) shown schematically in Fig. 1. Solutions of PBI in DMAc were loaded in a 2 mL hypodermic syringe and the solutions were delivered to the orifice of the stainless steel needle (of diameter 0.5 mm) by a syringe pump.

The electrospun products were collected onto a grounded aluminum foil-wrapped collector under the following experimental parameters:

**Fig. 1** Schematic diagram of a typical setup for electrospinning



- Solution concentration: 8, 10, 12, 14 and 16 % (w/v)
- Spinning voltages: 15, 20 and 25 kV
- Current: 20  $\mu$ A.
- Needle tip to collector distance: 16 cm.
- Solution flow rate: 0.2 mL/hr

The morphology of the electrospun fibers was observed under a scanning electron microscope (JEOL-JSM-6380LA, Japan) at an accelerating voltage of 20 kV, using secondary electrons for imaging. The specimens were gold sputtered by using a JFC 1600 autofine coater (JEOL, Japan) before being observed under the SEM.

### Statistical analysis

There are several relevant factors involved in the electrospinning process. These factors can be either operating conditions or the solution properties. DOE combines the relevant factors in different ways so as to determine which combination is the best. ANOVA is a major step in DOE and it has an impressive role on decision-making by analyzing the data. In this study, factorial design or two-way ANOVA with a confidence level of 99 % was used to quantify the effects of voltage, concentration, and voltage and concentration together on the electrospun fibers' diameters. Two-way ANOVA was chosen for this study, because, it has the ability to test several variables simultaneously and the level of every treatment is tested for all treatments;

also, it can account for the effect of noise factors. The optimum conditions for the fiber formation were determined experimentally and it was the input for the statistical study.

## Results and discussion

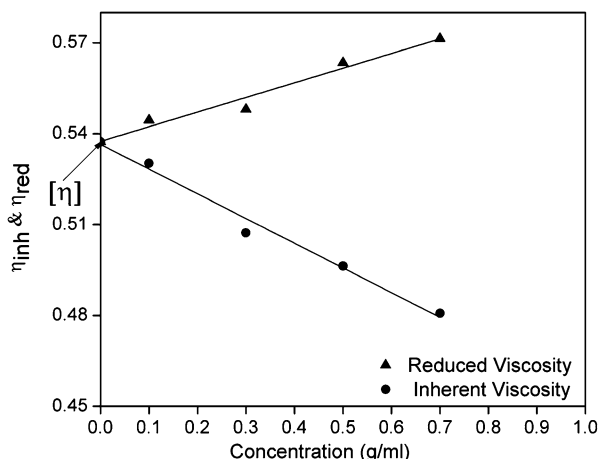
### Viscometry

Concentration versus reduced viscosity ( $\eta_r$ ) curve was plotted (Fig. 2) to obtain the value of inherent viscosity. Concentration versus inherent viscosity curve was also plotted. The intrinsic viscosity ( $[\eta]=[(\ln\eta_r)/C]_{C=0}$ ), for PBI was obtained from these plots and its value is 0.53, and the viscosity average molecular weight ( $\bar{M}_v$ ) is  $22,492 \text{ g}\cdot\text{mol}^{-1}$ .

### FTIR spectroscopy

In the infrared absorption spectrum of PBI (Fig. 3), absorption peaks at  $3229.4$  and  $3135.2 \text{ cm}^{-1}$  represent the stretching peaks of non-hydrogen bonded N-H and hydrogen bonded N-H groups, respectively [22]. Stretching mode of the aromatic C-H is assigned at  $3,063 \text{ cm}^{-1}$ . The peak  $2,357 \text{ cm}^{-1}$  is attributed to the stretching mode of the imidazole ring in the state of  $-\text{NH}^+$  [23]. The peaks at  $1990.7$  and  $2168.2 \text{ cm}^{-1}$  are due to interaction between substituted aromatic rings [24]. The peak at  $1621.7 \text{ cm}^{-1}$  is due to C=N stretching. The absorption peak at  $1432.4 \text{ cm}^{-1}$  arises from the in-plane deformation of benzimidazole, and the peak at  $1281.3 \text{ cm}^{-1}$  is from the breathing mode of imidazole rings [22]. The absorption peaks at  $852.1$  to  $680.5 \text{ cm}^{-1}$  indicate the aromatic C-H out of plane bending vibrations. The absence of carbonyl peaks between  $1,650$  and  $1,780 \text{ cm}^{-1}$  indicates the complete utilization of IPA and the closure of the imidazole ring during the synthesis. These results confirm the structure of PBI.

**Fig. 2** Concentration versus reduced and inherent viscosities



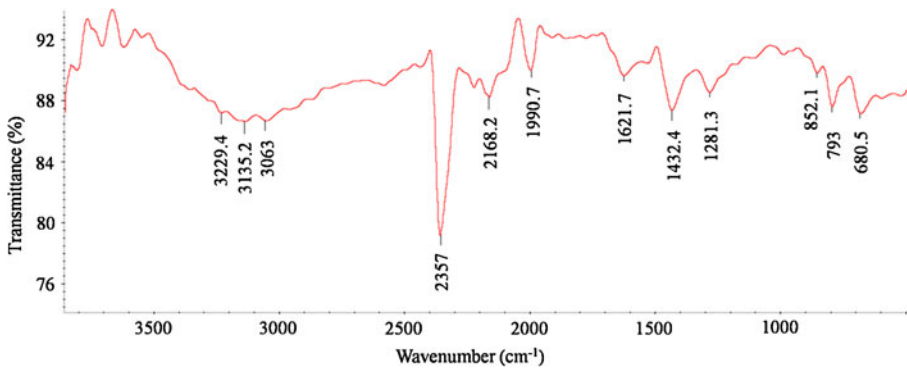


**Fig. 3** FTIR spectrum of PBI

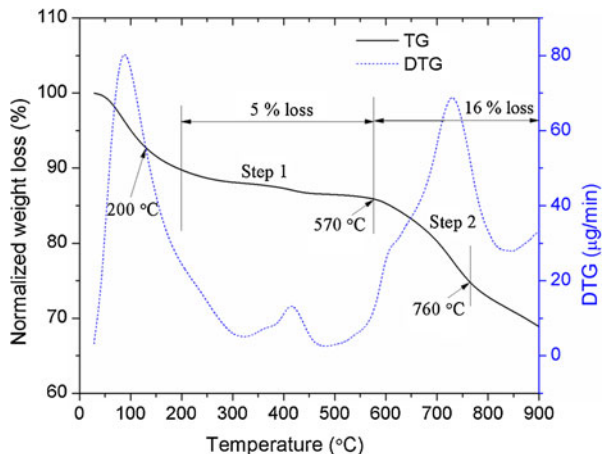
### Thermogravimetry

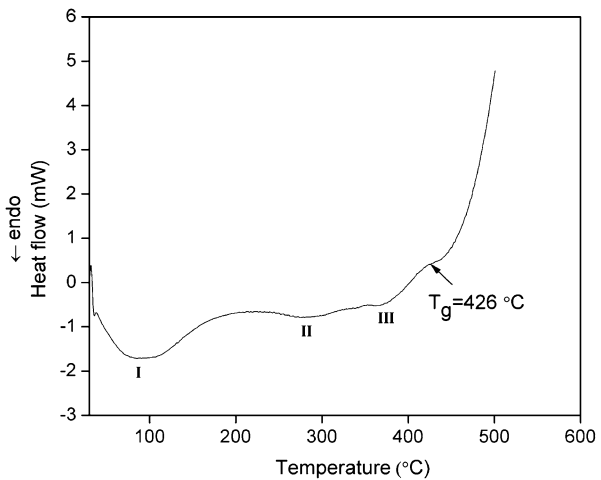
TGA curve (Fig. 4) reveals that PBI is stable up to 600 °C as reported in the literature [23]. PBI exhibits two steps in its degradation plot and the actual onset begins at about 200 °C; below 200 °C the absorbed moisture gets removed. The polymer progressively loses its weight from 200 °C to 570 °C with a 5 % weight loss; at this stage methane and water are the major volatile products. The second step in the degradation starts at around 570 °C and it drastically increases up to 760 °C and the major components released at this stage are methane, water, propene, hydrogen cyanide, benzene and benzonitrile. Above 760 °C hydrogen cyanide and nitrous oxide are the major volatile products [24]. In total, a 31 wt% weight loss is observed during this experiment.

### Differential scanning calorimetry

DSC analysis was carried out to determine the thermodynamic properties of PBI in the temperature range of 30–500 °C. From Fig. 5, it can be seen that the glass transition temperature ( $T_g$ ) of the PBI is around 426 °C. The endothermic peaks

**Fig. 4** TGA curve of PBI



**Fig. 5** DSC traces of PBI

below 370 °C (denoted as I, II and III) correspond to the evaporation of water and other volatile products, such as methane, propene, etc. This result is in agreement with that reported earlier in the literature [24, 25].

Effects of solution concentration and applied voltage on morphology and AFD of electrospun PBI fibers

#### *Effect of solution concentration*

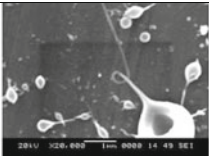
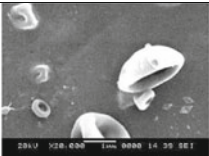
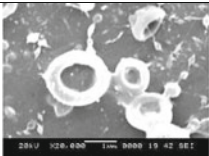
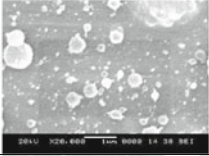
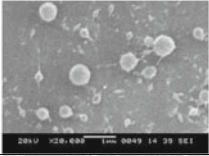
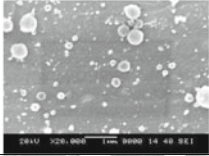
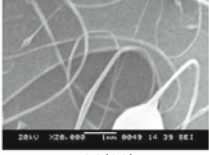
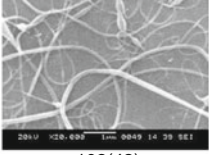
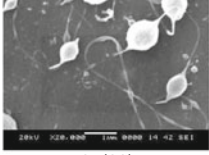
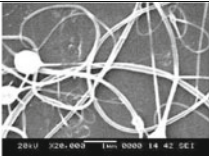
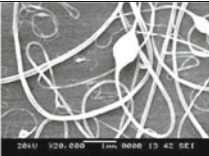
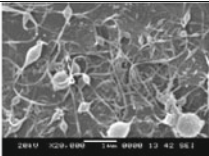
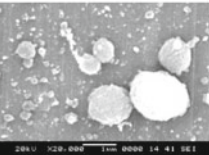
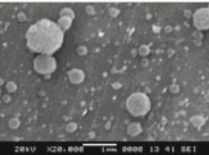
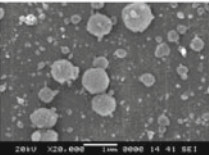
Several studies have demonstrated that solution concentration is one of the most important parameters in electrospinning. Morphology and AFD of electrospun nanofibers are dependent on solution viscosity and concentration [3–9]. If solution concentration is too low, droplets are produced instead of fibers, as the polymer solution jet breaks up into droplets; also, defects, such as beads can appear in fibers [26]. In this study, PBI solutions of five different concentrations (8, 10, 12, 14 and 16 %) were employed, to find the effect of concentration on fiber formation, morphology and fiber diameter. Table 1 shows the SEM micrographs of electrospun products of PBI at different solution concentrations under varying applied voltage. From the PBI solution of the lowest concentration (i.e., 8 %), fibers are not formed, but, only beads, droplets and cups are produced. At a concentration of 10 %, lot of beads along with some incipient fibers is obtained. Uniform fibers along with a small number of beads are produced at solution concentrations of 12 and 14 %. Solution concentration dictates the limiting boundaries for the formation of electrospun fibers through variations in viscosity and surface tension. At low solution concentration, droplets form due to the influence of surface tension, while higher concentration prohibits fiber formation due to higher viscosity. A high viscosity of polymer solution leads to formation of smooth, defect-free fibers [27, 28]. Solutions of low concentrations don't possess enough chain entanglements to withstand the electrostatic and Coulombic repulsive forces acting on an infinitesimal segment of a charged jet. Once the charged jet is broken up into smaller charged entities, surface tension will



minimize the surface area of the broken jets and, this in turn, leads to formation of discrete spheres. Increasing the solution concentration will enhance the formation of smooth and beaded fibers. At higher concentrations, the high enough chain entanglements would completely prevent the charged jet from breaking up. Interestingly, increasing polymer concentration will also result in fibers of larger diameters.

The SEM micrographs and diameter distribution histograms of PBI nanofibers obtained at the concentrations of 12 and 14 % are shown, respectively, in Figs. 6 and 7. The average diameter of the fibers increases with increasing solution concentration. This increase is a result of the increased viscoelastic forces that counteract the Coulombic repulsion forces. Electrospinning of the solution of concentration 16 % does not yield fibers, because, the solvent evaporated before the formation of jet; thereby it prohibited flow of the solution continuously to the capillary tip. The results

**Table 1** SEM (magnification 20,000× and scale bar=1 μm) images of the products of electrospinning of solutions containing different concentrations of PBI at different voltages

Concentration (w/v) %	Voltage (kV)		
	15	20	25
8			
10			
12			
14	91(23)	102(43)	95(38)
			
	106(48)	141(29)	56(6)
16			

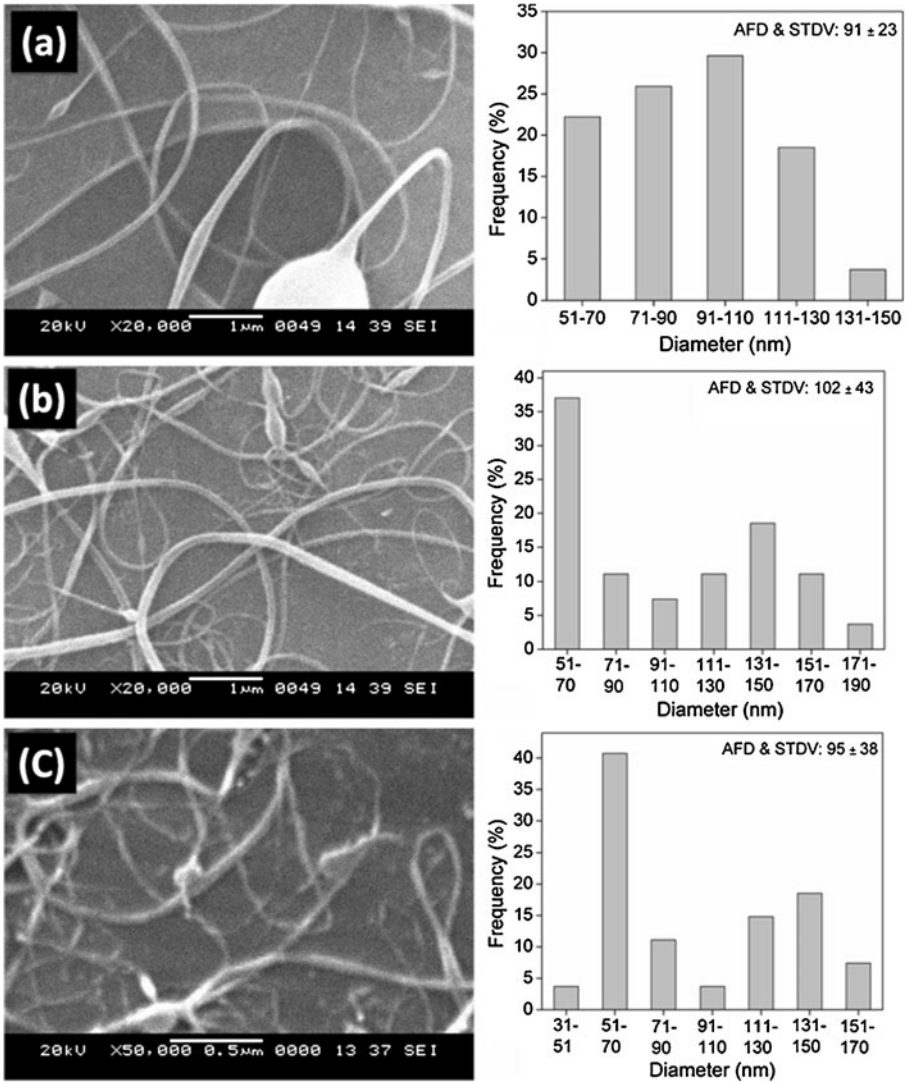


**Fig. 6** Scanning electron micrographs ((a) and (b) magnification 20,000 $\times$  and scale bar=1  $\mu$ m, c magnification 50,000 $\times$  and scale bar=0.5  $\mu$ m) and diameter histogram of PBI fibers at a concentration of 12 % (w/v) under varying applied voltage (for a fixed flow rate of 0.2 mL.hr<sup>-1</sup> and TCD of 16 cm): **a** at 15 kV, **b** at 20 kV, **c** at 25 kV. The values inside the diameter distribution histogram show the AFD along with the standard deviations

indicate that at a concentration of 16 %, fibers are absent and shapes of the beads were changed from cup shape to spherical shape (Table 1).

*Effect of applied voltage*

Literature review shows that the average diameter of fibers tends to decrease with increasing applied voltage. Increasing the applied voltage will increase the

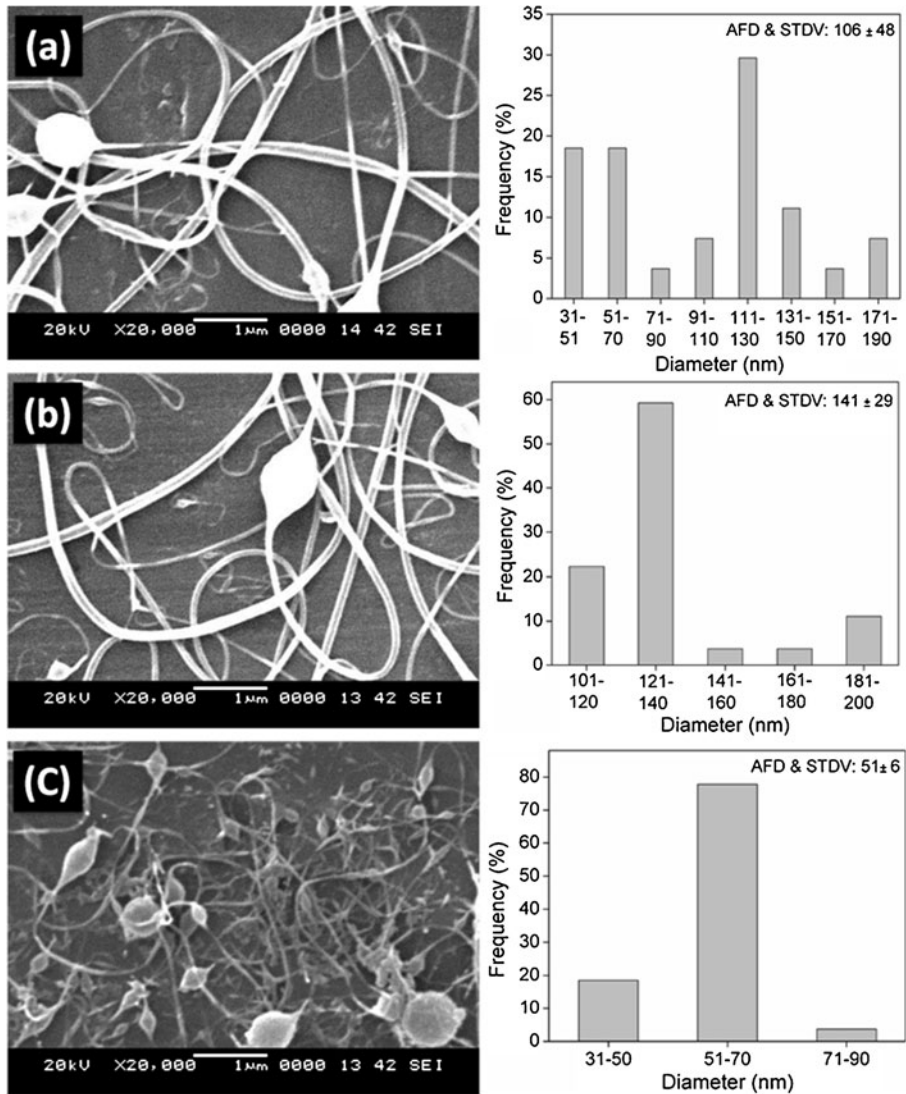
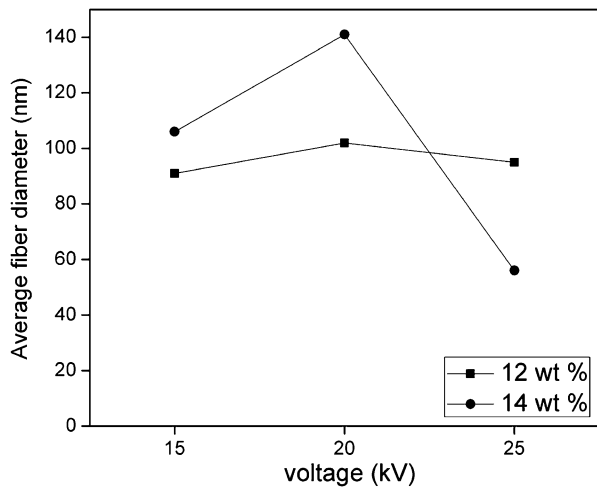


**Fig. 7** Scanning electron micrographs (magnification 20,000× and scale bar=1 μm) and diameter histogram of PBI fibers at a concentration of 14 % (w/v) under varying applied voltage (for a fixed flow rate of 0.2 mL.hr<sup>-1</sup> and TCD of 16 cm): a at 15 kV, b at 20 kV, c at 25 kV. The values inside the diameter distribution histogram show the AFD along with the standard deviations

electrostatic repulsive force on the fluid jet which might favor thinner fiber formation and also uniform fibers can be formed by increasing the applied voltage [28]. Table 1 shows the morphology of electrospun PBI fibers obtained at varied applied voltage from 15 kV to 25 kV under different solution concentrations and at a constant needle tip-to-collector distance of 16 cm. The results indicate that at low solution concentration (8 and 10 %) beads are formed irrespective of the applied voltage. Variation in voltage significantly affects the fiber diameter only at solution concentrations of 12 and 14 %.

**Fig. 8** Plot describing the relationship between AFD and applied voltage



The AFD is plotted as a function of the applied voltage at different concentrations (Fig. 8). It can be observed from the plot that the AFD increases when increasing the voltage from 15 kV to 20 kV. But, the AFD decreases with a further increase in the applied voltage (25 kV). When the applied voltage is increased, the jet velocity also increases and the removal of solution from the capillary tip is rapid. As the volume of the droplet on the spinneret becomes smaller, the Taylor cone shape gets oscillated and becomes asymmetrical. The jet originates from the liquid surface within the tip and beads can be observed. The AFD of the fibers electrospun at 25 kV was found to be smaller as compared to that obtained at lower voltages. The AFD tends to decrease with increasing applied voltage because of the simultaneous stretching effect of charged fibers [29, 30].

#### Statistical analysis using two-way ANOVA

Voltage at three levels (15, 20 and 25 kV) and concentration at two levels (12 and 14 %) were chosen for the ANOVA study, the reason was that nanofibers could be obtained only by using the combination of these voltages and concentrations as seen in the previous sections. The variations in the AFD produced by electrospinning can be either due to the change in the applied voltage or solution concentration, or the interaction of the voltage & concentration. The effect of voltage and concentration were considered as the ‘main effects’ and the combined effect of concentration and voltage as ‘interaction effect’.

In order to study the interaction effects among the process parameters, it was needed to vary all the factors simultaneously, which is called as full factorial design and is given in Table 2. Before stepping into ANOVA, in order to determine whether the two process parameters under consideration were interacting or not, a simple graphical tool called interaction graph was used and is shown in Fig. 9 [31]. In the interaction plot, if the lines are parallel, there is no interaction between the variables. On the other hand, if these are non-parallel, an interaction exists between them. Greater the degree of divergence from being parallel, the stronger the effect of

**Table 2** Full factorial design

Order	Factor		Average fiber diameter (nm)
	Concentration	Voltage	
1	12	15	91
2	12	20	102
3	12	25	95
4	14	15	106
5	14	20	141
6	14	25	56

interaction. Since the lines were not parallel in the interaction plot of voltage and concentration on fiber diameter (Fig. 9), it is possible to say that an effect of interaction exists on fiber diameter. ANOVA calculations were made using Table 3. The following equations are involved in the construction of the ANOVA table [32]:

$$SSC = V \sum_{j=1}^C (\bar{X}_j - \bar{X})^2 \tag{2}$$

$$SSV = C \sum_{i=1}^V (\bar{X}_i - \bar{X})^2 \tag{3}$$

$$SSI = n \sum_{i=1}^V \sum_{j=1}^C (\bar{X}_{ij} - \bar{X}_i - \bar{X}_j + \bar{X})^2 \tag{4}$$

**Main Effects Plot for Fiber Diameter**

Fitted Means

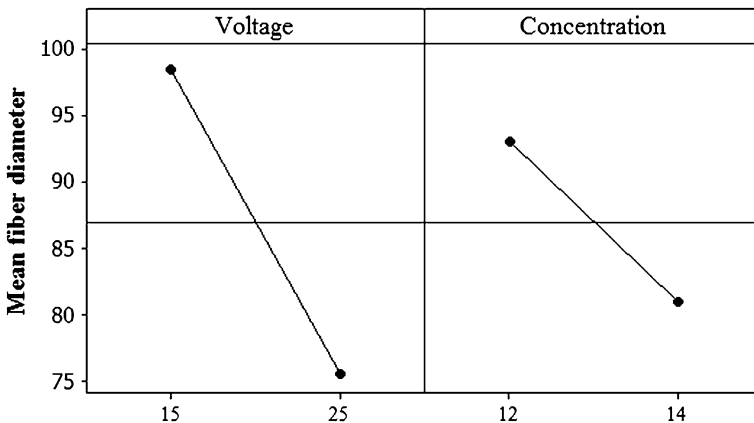


**Fig. 9** The interaction plot of voltage and concentration on fiber diameter

**Table 3** Construction of ANOVA table

Sources of variation	Sum of squares	Degrees of freedom	Mean square	F-statistics
Concentration	SSC	$a-1$	$MSC = \frac{SSC}{(a-1)}$	$F=MSC / MSE$
Voltage	SSV	$b-1$	$MSV = \frac{SSV}{(b-1)}$	$F=MSV / MSE$
Interaction of voltage & concentration	SSI	$(a-1)(b-1)$	$MSI=SSI / [(a-1)(b-1)]$	$F=MSI / MSE$
Error	SSE	$ab(n-1)$	$MSE=SSE / [ab(n-1)]$	–
Total	SST	–		

$$SSE = \sum_{i=1}^V \sum_{j=1}^C \sum_{k=1}^n (\bar{X}_{ijk} - \bar{X}_{ij}) \tag{5}$$

$$SST = \sum_{i=1}^V \sum_{j=1}^C \sum_{k=1}^n (\bar{X}_{ijk} - \bar{X})^2 \tag{6}$$

Where,

- SSC The sum of squares for the rows (concentration)
- SSV The sum of squares for the columns (voltage)
- SSI The sum of squares for the interactions (voltage & concentration)
- SSE The error of the sum of squares
- SST The total sum of squares
- ‘n’ The number of observed data in a cell
- ‘C=a’ The levels of column treatments
- ‘V=b’ The levels of row treatments
- ‘i’ The number of row treatment levels
- ‘j’ The column treatment levels
- ‘k’ The number of cells
- $\bar{X}_{ijk}$  Any observation
- $\bar{X}_{ij}$  The cell mean

**Table 4** ANOVA table for fiber diameter

Source of variation	Degrees of freedom	Sum of squares	Mean square	F-value	Contribution (%)
Concentration	1	934.56	934.56	0.75	1.85
Voltage	2	55942.51	27971.25	22.54	55.84
Interaction of voltage & concentration	2	42369.90	21184.95	17.07	42.29
Error	156	193570.05	1240.83	–	–
Total	161	292817.02			

Critical F values at 99 % confidence level :  $F_{0.01}(2,156)=4.7838$ ,  $f_{0.01}(1, 156)=6.8002$

$\bar{X}_i$	The level mean
$\bar{X}_j$	The treatment mean, and
$\bar{X}$	The mean of all the observations

The calculated  $F$  ( $F_{cal}$ ) values were compared with critical  $F$  ( $F_{cri}$ ) values.  $F_{cri}$  is less than  $F_{cal}$  at 99 % confidence level for the voltage, and interaction between the voltage and concentration indicating that these process parameters have a significant role in controlling the AFD. Table 4 is the ANOVA table for the fiber diameter. It is clear from Table 4 that the process parameters, voltage, and the interaction effect of voltage and concentration together, have a higher influence in controlling the AFD, whereas concentration alone does not have a significant impact on AFD.

## Conclusions

The results of this study show that ultrafine PBI fibers with average diameters ranging from 56 nm to 100 nm can be produced by carefully controlling the applied voltage and solution concentration. Ultrafine fibers could be obtained by electrospinning PBI solutions of concentrations 12 and 14 % at all the applied voltages employed in this study. From the statistical analysis it is proven that voltage, and the interaction between the voltage and concentration dominate over the concentration in controlling the fiber diameter. The PBI nanofibers could be potential candidates for advanced applications, such as proton exchange membranes and high temperature filters.

## References

- Greiner A, Wendorff JH (2007) Electrospinning: a fascinating method for the preparation of ultrathin fibers. *Angew Chem Int Ed* 46:5670–5703
- Huang Z-M, Zhang Y-Z, Kotaki M, Ramakrishna S (2003) A review on polymer nanofibers by electrospinning and their applications in nanocomposites. *Comp Sci Technol* 63:2223–2253
- Beachley V, Wen X (2009) Effect of electrospinning parameter on the nanofiber diameter and length. *Mat Sci Eng C* 29:663–668
- Heikkilä P, Harlin A (2008) Parameter study of electrospinning of polyamide-6. *Eur Polym J* 44:3067–3079
- Neo YP, Ray S, Easteal AL, Nikolaidis MG, Quek SY (2012) Influence of solution and processing parameters towards the fabrication of electrospun zein fibers with sub-micron diameter. *J Food Eng* 109:645–651
- Sukigara S, Gandhi M, Ayutsede J, Micklu M, Ko F (2003) Regeneration of bombyx mori silk by electrospinning—part I: processing parameters and geometric properties. *Polymer* 44:5721–5727
- Cui W, Li X, Zhou S, Weng J (2007) Investigation on process parameters of electrospinning system through orthogonal experimental design. *J Appl Polym Sci* 103:3105–3115
- Zamri MFMA, Zein SHS, Abdullah AZ, Basir NI (2012) The optimization of electrical conductivity using central composite design for polyvinyl alcohol/multiwalled carbon nanotube-manganese dioxide nanofiber composites synthesized by electrospinning. *J Appl Sci* 12:345–353
- Khan SP, Bhasin K, Newaz GM (2011) Optimizing process variables to control fiber diameter of electorspun polycaprolactone nanofiber using factorial design. *Mat Res Soc* 1316:6–15
- Dhara MG, Banerjee S (2010) Fluorinated high-performance polymers: poly(arylene ether)s and aromatic polyimides containing trifluoromethyl groups. *Prog Polym Sci* 35:1022–1077

11. Shabani I, Sadrabadi MMH, Asl VH, Soleimani M (2011) Nanofiber-based polyelectrolytes as novel membranes for fuel cell applications. *J Membrane Sci* 368:233–240
12. Serbezeanu D, Bubulac TV, Hamciuc C, Doroftei F (2010) Synthesis and characterization of new phosphorous-containing poly(ester imide)s. *High Perform Polym* 22:916–929
13. Zhang M, Wang Z, Zhang Y (2006) Preparation of polyimide nanofibers by electrospinning, international conference on MEMS, NANO and Smart Systems, 58–60
14. Moon SC, Choi J, Farris RJ (2008) Preparation of aligned polyetherimide fiber by electrospinning. *J Appl Polym Sci* 109:691–694
15. Nakata K, Kim SH, Ohkoshi Y, Gotoh Y, Nagura M (2007) Electrospinning of poly(ether sulfone) and evaluation of the filtration efficiency. *Soc Fiber Sci Technol* 63:307–312
16. Li Q, Jensen JO, Savinell RF, Bjerrum NJ (2009) High temperature proton exchange membranes based on PBIs for fuel cells. *Prog Polym Sci* 34:449–477
17. Shogbon CB, Brousseau J-L, Zhang H, Benicewicz BC, Akpalu YA (2006) Determination of the molecular parameters and studies of the chain conformation of PBI in DMAc/LiCl. *Macromolecules* 39:9409–9418
18. Kim J-S, Reneker DH (1999) PBI nanofiber produced by electrospinning. *Polym Eng Sci* 39:849–854
19. Ainla A, Brandell D (2007) Nafion®-PBI composite membranes for DMFC applications. *Solid State Ionics* 178:581–585
20. Billmeyer FW (1984) Text book of polymer science. John Wiley & Sons, USA
21. Andraday AL (2008) Science and technology of polymer nanofibers. John Wiley & Sons, USA, pp 23–26
22. Suryani, Liu Y-L (2009) Preparation and properties of nanocomposite membranes of PBI/sulfonated silica nanoparticles for proton exchange membranes. *J Membrane Sci* 332:121–128
23. Chen B, Luan D, Jiao G, Zhao D, Zhu Y (2009) Preparation of high temperature resistance PBI resin. *Front Chem China* 4:207–209
24. Coates J (2000) Encyclopedia of analytical chemistry. John Wiley & Sons, UK
25. Eguizábal A, Lemus J, Urbiztondo M, Garrido O, Soler J, Blazquez JA, Pina MP (2011) Novel hybrid membranes based on PBI and ETS-10 titanasilicate type material for high temperature proton exchange membrane fuel cells: a comprehensive study on dense and porous systems. *J Power Sources* 196:8994–9007
26. Zong X, Kim K, Fang D, Ran S, Hsiao BS, Chu B (2002) Structure and process relationship of electrospun bioabsorbable nanofiber membranes. *Polymer* 43:4403–4412
27. Deitzel JM, Kleinmeyer J, Harris D, Tan NC (2001) The effect of processing variables on the morphology of electrospun nanofibers and textiles. *Polymer* 42:261–272
28. Gu SY, Ren J, Vancso GJ (2005) Process optimization and empirical modeling for electrospun polyacrylonitrile (PAN) nanofiber precursor of carbon nanofibers. *Eur Polym J* 41:2559–2568
29. Shawon J, Sung C (2004) Electrospinning of polycarbonate nanofibers with solvent mixtures THF and DMF. *J Mater Sci* 39:4605–4613
30. Chowdhury M, Stylios G (2010) Effect of experimental parameter on the morphology of electrospun nylon-6 fibres. *Int J Basic Appl Sci* 10:116–131
31. Antony J (2003) Design of experiments for engineers and scientists. Elsevier Science & Technology, Burlington, Canada
32. Bass I (2007) Six sigma statistics with excel and minitab. McGraw-Hill, USA